



A Dual-Acting Nitric Oxide Donor and Phosphodiesterase 5 Inhibitor Promotes Wound Healing in Normal Mice and Mice with Diabetes

Maya Ben-Yehuda Greenwald¹, Carlotta Tacconi², Marko Jukic¹, Natasha Joshi¹, Paul Hiebert¹, Jürgen Brinckmann^{3,4}, Hermann Tenor⁵, Reto Naef⁵ and Sabine Werner¹

Chronic wounds affect a large percentage of the population worldwide and cause significant morbidity. Unfortunately, efficient compounds for the treatment of chronic wounds are yet not available. Endothelial dysfunction, which is at least in part a result of compromised nitric oxide production and concomitant reduction in cGMP levels, is a major pathologic feature of chronic wounds. Therefore, we designed and synthesized a compound with a unique dual-acting activity (TOP-N53), acting as a nitric oxide donor and phosphodiesterase 5 inhibitor, and applied it locally to full-thickness skin wounds in healthy and healing-impaired mice with diabetes. TOP-N53 promoted keratinocyte proliferation, angiogenesis, and collagen maturation in healthy mice without accelerating the wound inflammatory response or scar formation. Most importantly, it partially rescued the healing impairment of mice with genetically determined type II diabetes (*db/db*) by stimulating re-epithelialization and granulation tissue formation, including angiogenesis. In vitro studies with human and murine primary cells showed a positive effect of TOP-N53 on keratinocyte and fibroblast migration, keratinocyte proliferation, and endothelial cell migration and tube formation. These results demonstrate a remarkable healing-promoting activity of TOP-N53 by targeting the major resident cells in the wound tissue.

Journal of Investigative Dermatology (2021) 141, 415–426; doi:10.1016/j.jid.2020.05.111

INTRODUCTION

Wound repair is a complex process aiming at rapidly restoring skin integrity and function. It involves three overlapping phases—hemostasis and inflammation, new tissue formation, and tissue remodeling. This allows efficient regeneration of the epidermis, whereas the repair of the dermis results in scar formation (Gurtner et al., 2008; Martin, 1997; Werner and Grose, 2003). Inefficient healing is a frequent problem and may lead to ulcerative, chronic skin defects. The incidence of chronic wounds is increasing owing to the longer life expectancy and the growing number of patients with metabolic syndrome. This causes high morbidity and even mortality and enormous costs to the healthcare system (Eming et al., 2014; Sen et al., 2009).

Different factors can cause impaired healing, with local pressure effects, vascular insufficiency, and diabetes mellitus being the common causes (Eming et al., 2014). Chronic wounds include pressure ulcers, arterial and venous ulcers,

and diabetic foot ulcers, the latter being the major reason for leg amputation (Cash and Martin, 2016). Unfortunately, the therapeutic options for chronic wounds are yet unsatisfactory (Jones et al., 2018), which is at least in part due to the insufficient understanding of the complex underlying pathomechanisms.

Chronic wounds most often have a thick, nonmigratory epidermis and are characterized by an enhanced and prolonged inflammatory response, oxidative stress, reduced levels of bioactive GFs, impaired fibroblast proliferation and migration, abnormal extracellular matrix remodeling, and endothelial dysfunction (Eming et al., 2014; Falanga, 1992; Makrantonaki et al., 2017). The latter is at least in part a consequence of compromised nitric oxide (NO) production, with a concomitant reduction in the levels of cGMP (Kolluru et al., 2012).

The important role of NO in wound repair is reflected by the delayed wound closure and impaired angiogenesis in mice deficient for inducible or endothelial NO synthase (Lee et al., 1999; Lizarbe et al., 2008; Yamasaki et al., 1998). Moreover, systemic treatment of mice with an inhibitor for the inducible NO synthase caused impaired wound re-epithelialization (Stallmeyer et al., 1999), whereas the supplementation of wounds from rodents suffering from diabetes with NO-releasing compounds improved different aspects of the healing response (Masters et al., 2002; Weller and Finnen, 2006; Witte et al., 2002a, 2002b). In a clinical study, an NO-releasing medical device reduced the area of diabetic foot ulcers (Edmonds et al., 2018).

The enhancement of cGMP levels at the wound site has also shown beneficial effects. Thus, topical or systemic application of phosphodiesterase 5 (PDE5) inhibitors, for

¹Institute of Molecular Health Sciences, Department of Biology, ETH Zurich, Zurich, Switzerland; ²Institute of Pharmaceutical Sciences, Department of Chemistry and Applied Biosciences, ETH Zurich, Zurich, Switzerland; ³Department of Dermatology, University of Lübeck, Lübeck, Germany; ⁴Institute of Virology and Cell Biology, University of Lübeck, Lübeck, Germany; and ⁵Topadur Pharma AG, Schlieren, Switzerland

Correspondence: Sabine Werner, Institute of Molecular Health Sciences, Department of Biology, ETH Zurich, Otto-Stern-Weg 7, 8093 Zurich, Switzerland. E-mail: sabine.werner@biol.ethz.ch

Abbreviations: BEC, blood endothelial cell; GT, granulation tissue; KC, keratinocyte; NO, nitric oxide; PDE5, phosphodiesterase 5; SNAP, S-Nitroso-N-acetyl-DL-penicillamine; WE, wound epidermis

Received 12 December 2019; revised 12 April 2020; accepted 18 May 2020; accepted manuscript published online 27 June 2020; corrected proof published online 22 July 2020

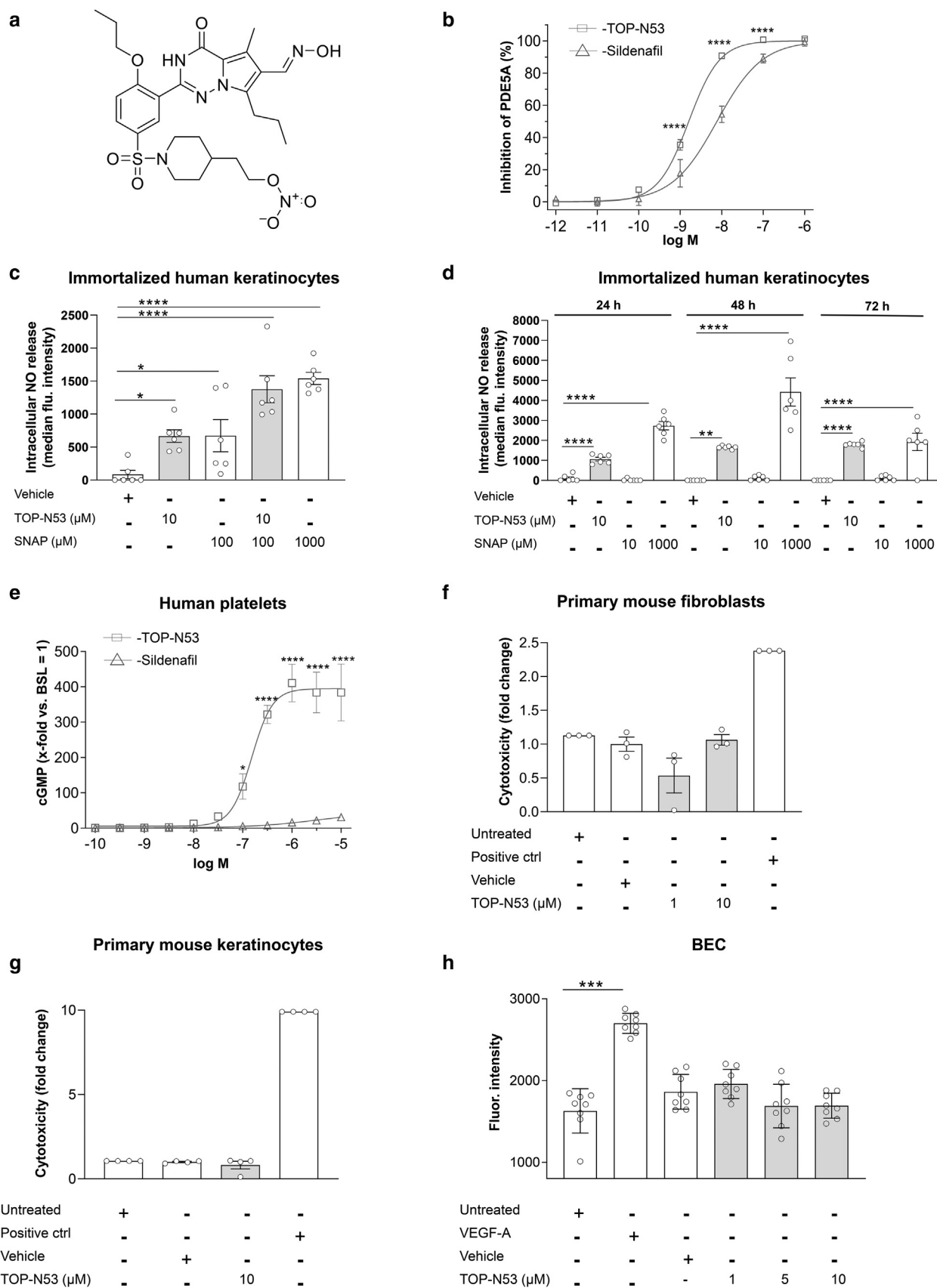


Figure 1. Characterization of TOP-N53. (a) The chemical formula of TOP-N53. (b) Inhibition of human PDE5A1 by TOP-N53 or sildenafil. $n = 19$ for TOP-N53 and 15 for sildenafil; $n = 3$ technical replicates of each. (c, d) Intracellular NO levels in HaCaT cells following TOP-N53 or SNAP treatment for (c) 24 h or (d) 24 h, 48 h, or 72 h. $n = 6$. (e) Increase in total cGMP in human platelets by TOP-N53 or sildenafil. $n = 3$ for TOP-N53; $n = 3$ for sildenafil. (f, g) LDH levels in the supernatant of primary mouse (f) fibroblasts or (g) KCs treated for 24 h with TOP-N53 or vehicle. Lysis buffer was used as a positive ctrl for cell death. Cultures

example, sildenafil (Viagra), which is well-known for its use in the treatment of erectile dysfunction, enhanced contraction, re-epithelialization, and tensile strength of rat wounds (Jamshidzadeh and Azarpira, 2011; Kulshrestha et al., 2019) and reduced pressure ulcer size in a few patients (Farsaei et al., 2015).

Despite these promising results, a comprehensive analysis of the *in vitro* and *in vivo* effects of NO donors and PDE5 inhibitors on the different cell types involved in wound repair has not been performed. Furthermore, a potential additive effect of NO supplementation and PDE5 inhibition has not been tested. Therefore, we designed and synthesized a compound that combines both activities, thereby increasing cGMP synthesis and at the same time preventing its degradation.

Here, we demonstrate a potent wound healing-promoting activity of such a compound through direct and indirect effects on the major skin-resident cells, suggesting its use for the treatment of skin ulcers.

RESULTS AND DISCUSSION

TOP-N53 is a dual-acting NO donor and PDE5 inhibitor

We designed and synthesized dual-acting compounds that act as NO donors and PDE5 inhibitors. Activation of the cGMP-producing enzyme soluble guanylate cyclase by NO and inhibition of the cGMP-degrading enzyme PDE5 is their cornerstone. They are expected to guarantee high-tissue cGMP levels, thereby improving wound microcirculation. This is particularly important in diabetic ulcers, which are characterized by low vascularity and capillary density (Dinh and Veves, 2005; Okonkwo and DiPietro, 2017), often as a consequence of compromised NO production and reduced cGMP levels (Campbell et al., 2013; Eming et al., 2014; Kolluru et al., 2012).

TOP-N53 (Figure 1a) (Naef and Tenor, 2017), a bifunctional NO-releasing organic nitrate and selective PDE5 inhibitor, was specifically designed for local administration. It potently inhibited PDE5 with a half-maximal inhibitory concentration of 1.6 nM. This value is approximately five-fold lower than that of the PDE5 inhibitor sildenafil (Figure 1b), indicating its higher potency. Intracellular NO levels increased upon a 24-hour treatment of immortalized human keratinocytes (KCs) (HaCaT cells) with 10 μ M TOP-N53 as assessed by measurement of the fluorescence of the product of 3-amino-4-(*N*-methylamino)-2',7'-difluorofluorescein that is formed in the presence of NO. Importantly, a 10-fold higher concentration of the NO-releasing compound *S*-nitroso-*N*-acetyl-DL-penicillamine (SNAP) was required to generate similar levels of NO, and cotreatment with TOP-N53 and SNAP had an additive effect (Figure 1c). The fluorescence intensity was stable for up to 72 hours after TOP-N53 treatment, whereas the fluorescence induced by 1 mM SNAP already started to decline at this time point (Figure 1d). Treatment of human platelets, which express PDE5 (Gresele et al., 2011), with TOP-N53 increased the

levels of cGMP in a concentration-dependent and time-dependent manner and was significantly more potent than sildenafil (Figure 1e and Supplementary Figure S1a). Importantly, TOP-N53 had no toxic effects on primary mouse fibroblasts and KCs, human blood endothelial cells (BECs), and human HaCaT KCs (Figure 1f–h and Supplementary Figure 1b).

TOP-N53 promotes different parameters of wound healing in healthy mice

To investigate the wound healing-promoting potential of TOP-N53, we first analyzed full-thickness excisional wounds at day 5 after wounding in healthy mice. This time point was chosen because it represents the peak of re-epithelialization and granulation tissue (GT) formation (Werner and Grose, 2003). TOP-N53 or vehicle was injected intradermally at the wound edge immediately after wounding and at day 3 after injury (Supplementary Figure S1c). The treated mice neither showed weight loss (Supplementary Figure S1d) nor obvious signs of pain or irritation. Only 8% of the wounds in the vehicle-treated but 26% of the wounds in TOP-N53-treated mice were closed at day 5 (Figure 2a and b). However, histomorphometric analysis (Supplementary Figure S1e) of H&E-stained or Herovici-stained wound sections did not reveal a significant increase in wound re-epithelialization (Figure 2a and c). Furthermore, the thickness of the wound epidermis (WE), the length of the epithelial tongue that reflects the migration distance, and the GT area were similar in mice of both treatment groups (Figure 2d–f). A minor increase in wound contraction was seen in TOP-N53-treated wounds (Figure 2g). Similar results were obtained with 10-fold higher amounts of TOP-N53 (Supplementary Figure S1f–i).

Because wound repair is highly optimized in healthy mice, any positive effect of TOP-N53 may not be visible by histomorphometric analysis. Therefore, we performed a more detailed characterization of the wound tissue. Remarkably, TOP-N53 strongly promoted cellular proliferation in the WE and GT (Figure 2h–j). Biochemical analyses revealed that the total collagen content was mildly but nonsignificantly reduced in TOP-N53-treated wounds (Figure 2k). However, collagen crosslinking was significantly increased (Figure 2l–m), indicating accelerated collagen maturation. Consistent with the biochemical data, Herovici staining, which stains young and mature collagen fibers in blue and purple, respectively, did not reveal obvious differences in the collagen-positive area between treatment groups, whereas TOP-N53-treated wounds showed a slight increase in the ratio of mature to young collagen (Figure 2a and n–o).

The area of GT that stained positive for the vascular endothelial cell marker Meca32 was significantly larger in the TOP-N53-treated wounds (Figure 2p and q), whereas vessel size was not altered (Supplementary Figure 1j). Vessel maturation at day 5 after wounding was also mildly but significantly increased as illustrated by the larger percentage

← from $n = 3-4$ mice. (h) MUH fluorimetry analysis of human primary BEC treated for 72 hours with TOP-N53 or vehicle. Negative ctrl: starvation medium; positive ctrl: 20 ng/ml VEGF-A. $n = 8$. BEC, blood endothelial cell; BSL, baseline; ctrl, control; Fluor., fluorescence; flu, fluorescence; h, hour; KC, keratinocyte; LDH, lactate dehydrogenase; MUH, 4-methylumbelliferyl heptanoate; NO, nitric oxide; PDE5, phosphodiesterase 5; SNAP, *S*-Nitroso-*N*-acetyl-DL-penicillamine.

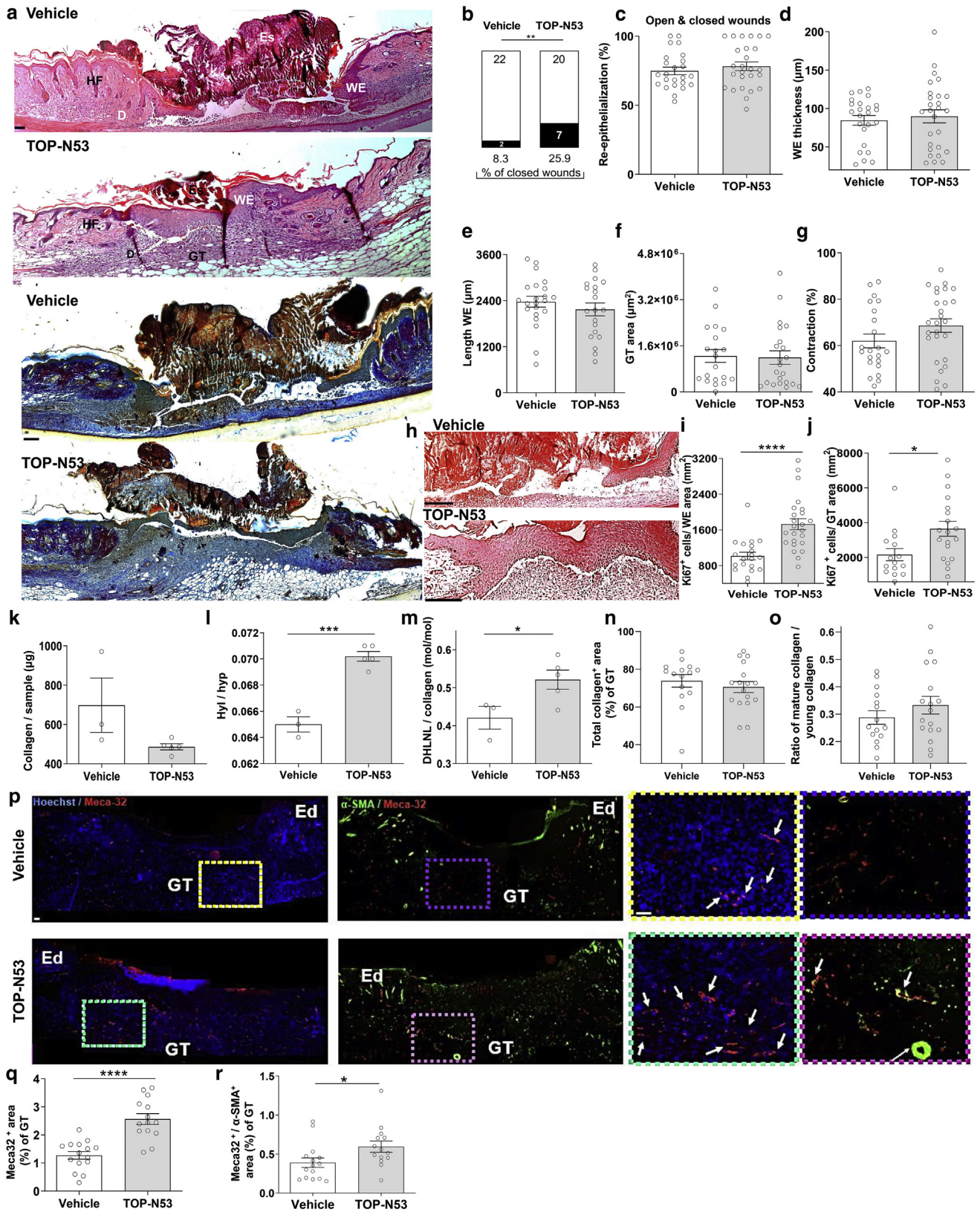


Figure 2. TOP-N53 promotes different aspects of wound healing in healthy mice. (a) Photomicrographs of H&E (top) and Herovici-stained (bottom) sections from 5-day wounds treated with 0.001 pmol TOP-N53 per injection day or vehicle. (b) Number and percentages of open (white bars) and closed (black bars) 5-day wounds. (c) Percentage of wound re-epithelialization, including open and closed wounds. n = 14–15 mice; n = 24–27 wounds. Average (d) thickness and (e) length of the WE. n = 14–15 mice; n = 20–22 wounds. (f) Area of GT. n = 14–15 mice; n = 20–22 wounds. (g) Percentage of wound contraction. n = 14–15 mice; n = 22–27 wounds. (h) Representative photomicrographs of wound sections stained for Ki67. (i, j) Ki67⁺ cells per mm² (i) WE or (j) GT. n = 14–15 mice; n = 15–25 wounds. (k–m) Amount of total (k) collagen per wound sample (μg), (l) Hyl-to-hyp ratio, and (m) DHLNL-to-collagen ratio. n = 3–5 mice. (n) Percentage of collagen-positive GT area and (o) ratio of mature (purple)-to-young collagen (blue) based on Herovici staining. n = 9–10 mice, n = 15–17

of vessels surrounded by α -smooth muscle actin-expressing vascular smooth muscle cells (Figure 2p and r). No obvious difference in the number of myofibroblasts was detected for the different treatment groups as reflected by a similar area covered by α -smooth muscle actin-positive cells outside the vessels (Supplementary Figure S1k). The effect of TOP-N53 on wound angiogenesis was verified by staining for CD31, which is expressed in both vascular and lymphatic endothelial cells (Supplementary Figure S2a and b). In addition, three consecutive intradermal injections of TOP-N53 within 1 week into nonwounded mouse ear skin increased the number of blood vessels (Supplementary Figure S2c and d).

TOP-N53 did not provoke an excessive wound inflammatory response. Thus, flow cytometry showed no differences in the number of total immune cells, total myeloid cells, monocytes, macrophages, neutrophils, dendritic cells, or T cells between both treatment groups (Supplementary Figure S2e and f). The only difference was a slight increase in macrophages in unwounded skin of TOP-N53-treated mice, indicating a minor proinflammatory activity of the compound. The number of live cells in normal and wounded skin was not affected by TOP-N53, demonstrating a lack of toxicity. Finally, the expression of the proinflammatory cytokines TNF- α , IL-6, and IL-1 β was not affected (Supplementary Figure S2g-i).

The effect of TOP-N53 on KC proliferation was already observed at day 3 after wounding, whereas no effect on body weight, angiogenesis, and different histomorphometric parameters was seen at this early stage (Supplementary Figure S3a-i).

Taken together, these results demonstrate that TOP-N53 promotes KC proliferation, angiogenesis, and collagen maturation in wounded skin but does not further enhance the normal wound inflammatory response. Therefore, it seems to be most efficient during the proliferation phase, when inducible NO synthase levels already decline and NO is mainly produced by endothelial NO synthase (Schwentker and Billiar, 2003).

TOP-N53 does not promote scarring

At day 14 after wounding (Supplementary Figure S1c), all wounds were closed in TOP-N53-treated and vehicle-treated mice (Figure 3a). TOP-N53-treated wounds had a thicker WE, but there were no significant differences in wound contraction and late GT area (Figure 3a-d). The number of Ki67-positive cells in the WE of TOP-N53-treated mice was still mildly elevated, whereas the number of proliferating cells in the GT was similar in both treatment groups (Figure 3e and f). Importantly, total collagen content, percentage of collagen among total protein, and collagen crosslinking (Figure 3g-j) were similar in both treatment groups at this time point, suggesting that the positive effect of TOP-N53 on wound healing does not result in enhanced scarring. In the future, it should be determined whether and to what extent TOP-N53 affects the mechanical properties of the healed wounds. The absence of a profibrotic fibroblast phenotype was confirmed in vitro because a 24-hour

treatment of cultured primary fibroblasts with TOP-N53 did not affect the gene expression of *Tgfb1*, *Fn1*, and *Col1a1* and *Col1a2* (Figure 3k-n). The lack of a profibrotic effect of TOP-N53 is consistent with the reduced expression of NO synthase in hypertrophic scars (Wang et al., 1997) and the inhibition of bleomycin-induced lung fibrosis by PDE5A inhibitors and NO donors (Davis et al., 2000; Hemnes et al., 2008; Kilic et al., 2014).

TOP-N53 promotes wound re-epithelialization and angiogenesis in mice with diabetes

We next tested the therapeutic efficacy of TOP-N53 in mice with genetically determined type II diabetes (*db/db*), which are commonly used as a model for impaired wound healing (Tsuboi and Rifkin, 1990). Injections were given immediately after wounding and on day 3 for analysis on day 5 or immediately after wounding and on days 3 and 5 for analysis on day 8 after wounding (Supplementary Figure S1c). Because of the impaired wound healing in mice with diabetes and the reduction in endogenous NO levels as a consequence of NO synthase dysfunction (Cai et al., 2005), we used a higher dose of TOP-N53 than in the experiments with healthy mice.

TOP-N53 did not affect body weight (Supplementary Figure S4a and b). The majority of the wounds of both treatment groups were still open on day 5 but closed on day 8 (Figure 4a and b). However, histomorphometric analysis of the 5-day wounds revealed significantly enhanced re-epithelialization of the TOP-N53-treated wounds (Figure 4c). This increase seems to result from enhanced KC migration as reflected by the length of the WE and enhanced KC proliferation as reflected by the thickness of the WE (Figure 4d and e). By contrast, wound contraction was not significantly affected (Figure 4f). The area of GT was similar in mice of both treatment groups on day 5 after wounding, whereas a mild but nonsignificant increase was observed on day 8 in the TOP-N53-treated mice (Figure 4g). The number of proliferating cells in the epidermis was significantly higher in TOP-N53-treated wounds at both time points, and a strong increase in proliferating cells was also seen in the GT on day 8 (Figure 4h-j). The positive effect of TOP-N53 on wound repair was confirmed by semiquantitative wound scoring, which demonstrated a significant increase in re-epithelialization on day 5 and a mild acceleration of GT maturation at both time points (Supplementary Figure S4c and d).

On day 8, the total GT area that stained positive for the vascular marker CD31 was mildly increased in TOP-N53-treated wounds, and this difference was significant for the GT at the wound edge (Figure 4k-m). Mean vessel size was similar in TOP-N53-treated and vehicle-treated diabetic wounds (Supplementary Figure S4e). The α -smooth muscle actin-positive area outside of vessels was slightly lower in TOP-N53-treated wounds (Supplementary Figure S4f). TOP-N53 treatment did not affect the number of different immune cells in 5-day wounds (Supplementary Figure S4g), whereas the noninjured skin adjacent to the wounds of TOP-

wounds. (p) Photomicrographs of wound sections stained for Meca-32 (red) and α -SMA (green) and counterstained with Hoechst (blue). (q, r) Percentage of GT area positive for (q) Meca32 or (r) Meca32 and α -SMA. n = 14–15 mice. Bars = 100 μ m. D, dermis; DHLNL, dihydroxylysinoxonoleucine; Ed, wound edge; Es, eschar; GT, granulation tissue; HF, hair follicle; Hyl, hydroxylysine; hyp, hydroxyproline; α -SMA, smooth muscle actin- α ; WE, wound epidermis.

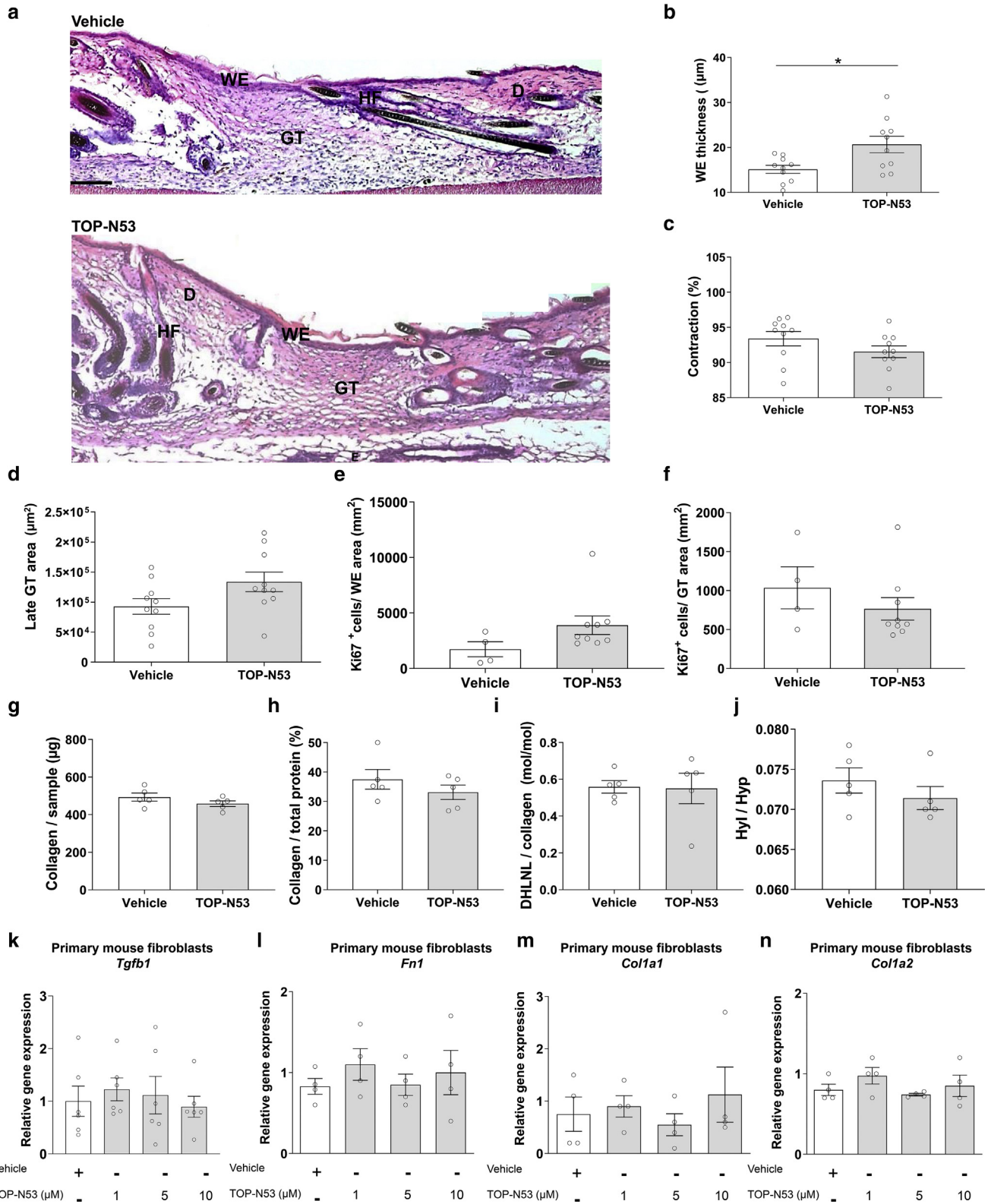


Figure 3. TOP-N53 does not enhance scarring. (a) Photomicrographs of H&E-stained sections from 14-day wounds treated with 0.001 pmol TOP-N53 per injection day or vehicle. Scale Bars = 100 μm . (b) The average thickness of the WE. $n = 5$ mice; $n = 10$ wounds. (c) Percentage of wound contraction. $n = 5$ mice; $n = 10$ wounds. (d) Area of late GT and/or early scar tissue. $n = 5$ mice; $n = 10$ wounds. (e, f) Ki67^+ cells per mm^2 (e) WE or (f) GT. $n = 4-5$ mice; $n = 4-9$ wounds. (g) Total collagen per wound sample (μg), (h) total collagen per total protein, (i) DHLNL-to-total collagen ratio, and (j) Hyl-to-Hyp ratio in the wound samples. $n = 5$ mice. (k-n) RT-qPCR of RNA from mouse fibroblasts treated for 24 hours with TOP-N53 or vehicle for expression of *Tgfb1*, *Fn1*, *Col1a1*, or *Col1a2* relative to *Rps29*. Cultures from $n = 4-6$ mice. D, dermis; DHLNL, dihydroxylysineonorleucine; GT, granulation tissue; HF, hair follicle; Hyl, hydroxylysine; Hyp, hydroxyproline; WE, wound epidermis.

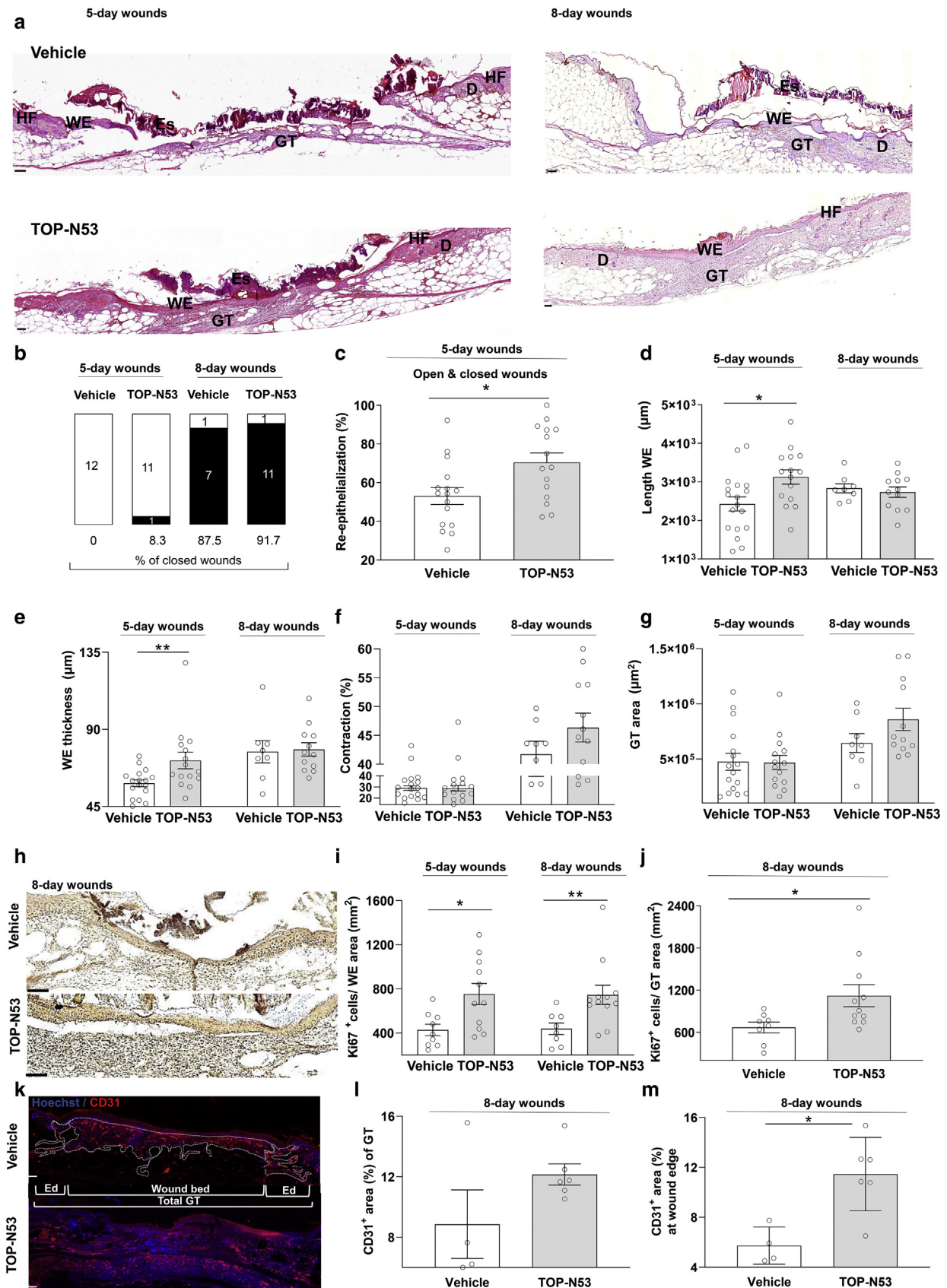


Figure 4. TOP-N53 promotes different aspects of wound healing in mice with diabetes. (a) Photomicrographs of H&E-stained sections from 5-day and 8-day wounds of *db/db* mice treated with 0.2 nmol TOP-N53 per injection day or vehicle. (b) Number and percentages of open (white bars) and closed (black bars) 5-day and 8-day wounds. (c) Percentage of wound re-epithelialization in 5-day wounds, including open and closed wounds. $n = 9-11$ mice; $n = 15-16$ wounds. (d) Length and (e) average thickness of the WE. $n = 9-11$ mice and $n = 15-18$ wounds (5-day wounds); $n = 4-6$ mice and $n = 8-12$ wounds (8-day wounds).

N53–treated mice had slightly higher numbers of different myeloid cells.

Taken together, these results demonstrate that TOP-N53 also promotes wound re-epithelialization and angiogenesis in mice with diabetes without increasing wound inflammation.

TOP-N53 directly induces healing-promoting activities in KCs and fibroblasts

Consistent with the increased KC proliferation in healing wounds, a 24-hour treatment of primary mouse KCs with TOP-N53 enhanced their proliferation rate (Figure 5a and Supplementary Figure S5a). The effect was reversed in the presence of the NO scavenger 2-(4-carboxyphenyl)-4,4,5,5-tetramethylimidazoline-1-oxyl-3-oxide (Figure 5a). However, treatment with this compound even suppressed the proliferation rate of vehicle-treated KCs, reflecting the requirement of basal NO levels for efficient proliferation of KCs. Similar results were obtained in scratch wounding migration assays (Figure 5b). The differences between vehicle and TOP-N53 in KC proliferation and migration did not reach statistical significance when analyzed together with the 2-(4-carboxyphenyl)-4,4,5,5-tetramethylimidazoline-1-oxyl-3-oxide effect by two-way ANOVA test but was significant when data from vehicle-treated and TOP-N53–treated cells were analyzed independently of the inhibitor using Mann–Whitney test (Figure 5a, $**P = 0.0087$ and 5b, $**P = 0.0002$).

The dose-dependent stimulation of KC migration by TOP-N53 and the requirement of NO for efficient migration were verified with HaCaT KCs (Supplementary Figure S5b) and with primary human KCs (Figure 5c). Interestingly, similar concentrations of sildenafil or SNAP or a combination of both were less potent. Only a five-fold higher concentration of SNAP, or a combination of SNAP and sildenafil had a significant effect on migration (Figure 5c).

These results are consistent with the positive effect of NO on KC proliferation and migration in vitro (Krischel et al., 1998; Zhan et al., 2015) and on wound re-epithelialization in vivo (Stallmeyer et al., 1999). However, NO at high doses inhibited these processes (Krischel et al., 1998), indicating the need for appropriate dosing of NO donors at the wound site. The PDE5 inhibitory activity of TOP-N53 is probably of minor importance for KC function because these cells express only very low levels of PDE5 and of different guanylate cyclase subunits in vivo (Joost et al., 2016; Sennett et al., 2015).

The proliferation rate of primary mouse fibroblasts was not affected by TOP-N53 (Supplementary Figure S5c), but the migration of immortalized and primary mouse and human fibroblasts was strongly accelerated in an NO-dependent manner (Supplementary Figure S5d and Figure 5d–e). This result is consistent with the promigratory effect of NO for fibroblasts (Han et al., 2012). Sildenafil, SNAP, or combinations of both were less potent

(Figure 5e). TOP-N53 also promoted the capability of fibroblasts to contract a collagen gel (Figure 5f). However, this was not reflected by a significant increase in wound contraction or myofibroblast numbers in the skin wounds (see above).

Because paracrine stimulation of KCs by fibroblast-derived mitogens such as HGF and FGF7, promotes wound re-epithelialization (Werner et al., 2007), we treated mouse primary fibroblasts for 24 hours with TOP-N53 and found a strong increase in the mRNA levels of both factors (Figure 5g and h). This result suggests that TOP-N53 may also indirectly promote KC migration and proliferation at the wound site. By contrast, TOP-N53 did not affect the mRNA levels of the fibroblast mitogens activin A (encoded by the *Inhba* gene) or *Pdgfa*, and the expression of *Tgfb1* and *Tgfb3* was even mildly reduced (Supplementary Figure S5e–h).

Overall, these results demonstrate that TOP-N53 directly affects fibroblast and KC functions, which may be potentiated by a paracrine effect on KCs.

TOP-N53 promotes endothelial cell migration and tube formation

Finally, we determined whether TOP-N53 directly affects endothelial cells and thereby promotes angiogenesis as seen in our wound healing and ear injection studies. TOP-N53 had no effect on the endothelial cell number (Figure 1h), but it significantly accelerated the migration of BEC and human umbilical vein endothelial cells, which was reversed by NO scavenging (Figure 6a and Supplementary Figure S6a and b). The difference between vehicle and TOP-N53 was statistically significant when data from vehicle-treated and TOP-N53–treated cells were analyzed independently of the inhibitors using Mann–Whitney test (Figure 6a, $*P = 0.049$; $*P = 0.0104$; $*P = 0.0207$ for TOP-N53 at 1 μM ; 2.5 μM ; and 5 μM , respectively). This result is consistent with the promigratory effect of NO-generating compounds for endothelial cells (Murohara et al., 1999; Ziche et al., 1994). However, SNAP or sildenafil or the combination of both did not significantly promote the migration of BEC under our experimental conditions (Figure 6b). Five-fold higher concentrations of sildenafil or SNAP were used in this experiment because of the approximate five-fold difference in the half-maximal inhibitory concentration of TOP-N53 and sildenafil to inhibit PDE5 (Figure 1b).

TOP-N53 strongly promoted tube formation by BEC and human umbilical vein endothelial cells as revealed by a significant increase in the number of branches, total tube length, and the number of junctions, which was reversed by 2-(4-carboxyphenyl)-4,4,5,5-tetramethylimidazoline-1-oxyl-3-oxide (cPTIO) (Figure 6c–i and Supplementary Figure S6c–h). The proangiogenic activity of TOP-N53 may also involve its PDE5 inhibitory activity because positive effects on endothelial cell migration and tubular

(f) Percentage of wound contraction. $n = 9–11$ mice and $n = 15–17$ wounds (5-day wounds); $n = 4–6$ mice and $n = 8–12$ wounds (8-day wounds). (g) Area of GT. $n = 9–11$ mice and $n = 14–16$ wounds (5-day wounds); $n = 4–6$ mice and $n = 8–12$ wounds (8-day wounds). (h) Photomicrographs of Ki67-stained wound sections. (i, j) Ki67⁺ cells per mm² (i) WE or (j) GT. $n = 6$ mice and $n = 9–11$ wounds (5-day wounds); $n = 4–6$ mice and $n = 8–12$ wounds (8-day wounds). (k) Photomicrographs of CD31-stained wound sections (red) and counterstained with Hoechst (blue). (l, m) Percentage of CD31-positive total (l) GT area or GT area at the (m) Ed. $n = 4–6$ mice. Scale Bars = 100 μm . D, dermis; Ed, wound edge; Es, eschar; GT, granulation tissue; HF, hair follicle; WE, wound epidermis.

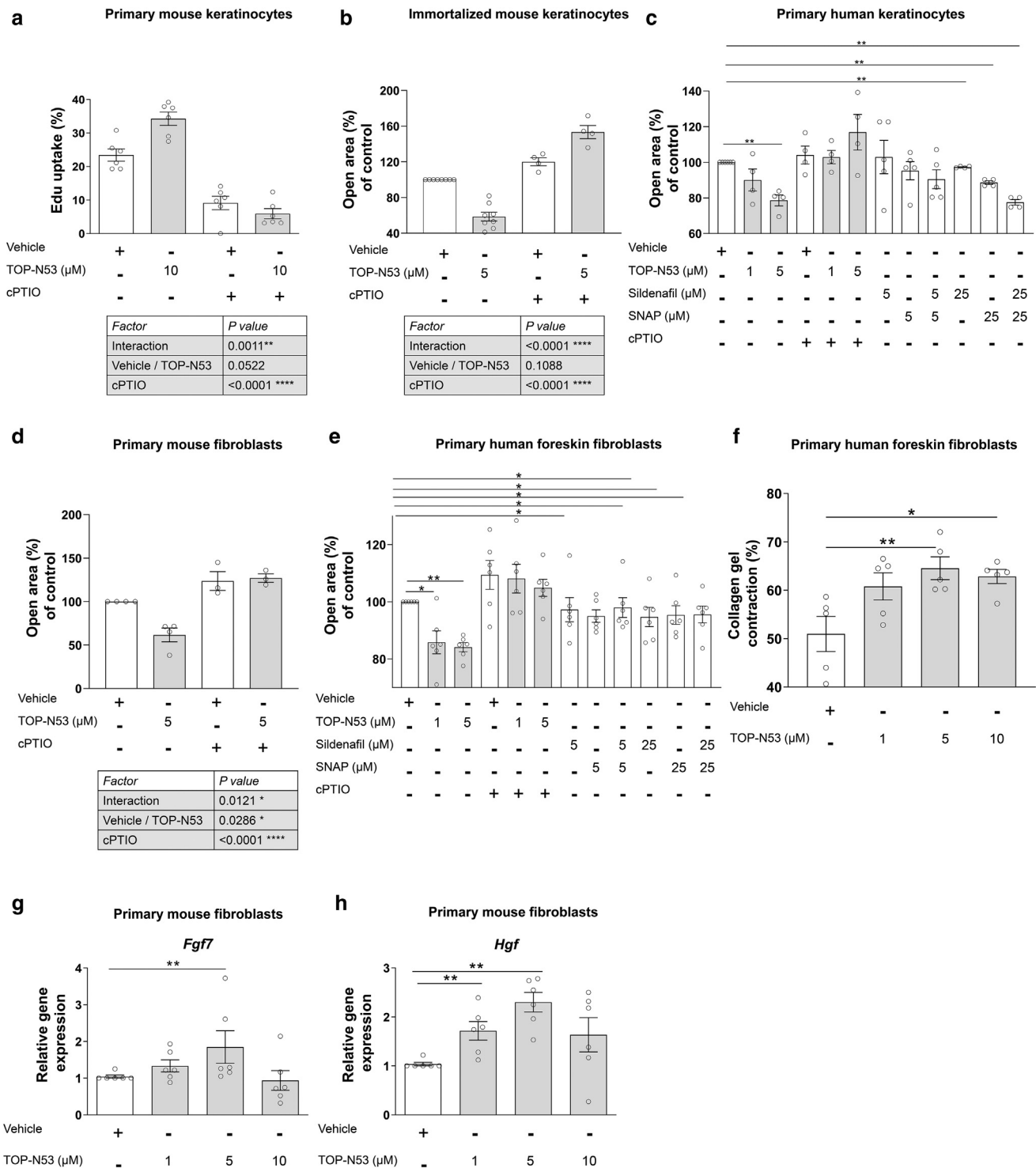


Figure 5. TOP-N53 induces healing-promoting activities in KCs and fibroblasts. (a) EdU uptake of primary mouse KCs treated for 24 hours with 10 μM TOP-N53 or vehicle in the presence or absence of cPTIO. $n = 6$ mice. (b) Scratch wound closure by immortalized mouse KCs treated for 24 h with 5 μM TOP-N53 or vehicle in the presence or absence of cPTIO. $n = 4-8$ mice. (c) Scratch wound closure by primary human foreskin KCs treated for 50 h with TOP-N53 or vehicle in the presence or absence of cPTIO or with sildenafil and/or SNAP. $n = 4-5$ from one donor. (d) Scratch wound closure by primary mouse fibroblasts treated for 50 h with 5 μM TOP-N53 or vehicle in the presence or absence of cPTIO. $n = 3-4$ mice. (e) Scratch wound closure by primary human foreskin fibroblasts treated for 12 h with TOP-N53 or vehicle in the presence or absence of cPTIO or with sildenafil and/or SNAP. $n = 6$ from two donors. (f) Collagen gel contraction by primary human foreskin fibroblasts treated with TOP-N53 or vehicle for 1.5 hours. $n = 5$ technical replicates. (g, h) RT-qPCR of RNA from primary mouse fibroblasts treated for 24 hours with TOP-N53 or vehicle for *Fgf7* or *Hgf* relative to *Rps29*. Cultures from $n = 6$ mice. cPTIO, 2-(4-carboxyphenyl)-4,4,5,5-tetramethylimidazole-1-oxyl-3-oxide; EdU, 5-ethynyl-2 deoxyuridine; h, hour; KC, keratinocyte; SNAP, S-Nitroso-N-acetyl-DL-penicillamine.

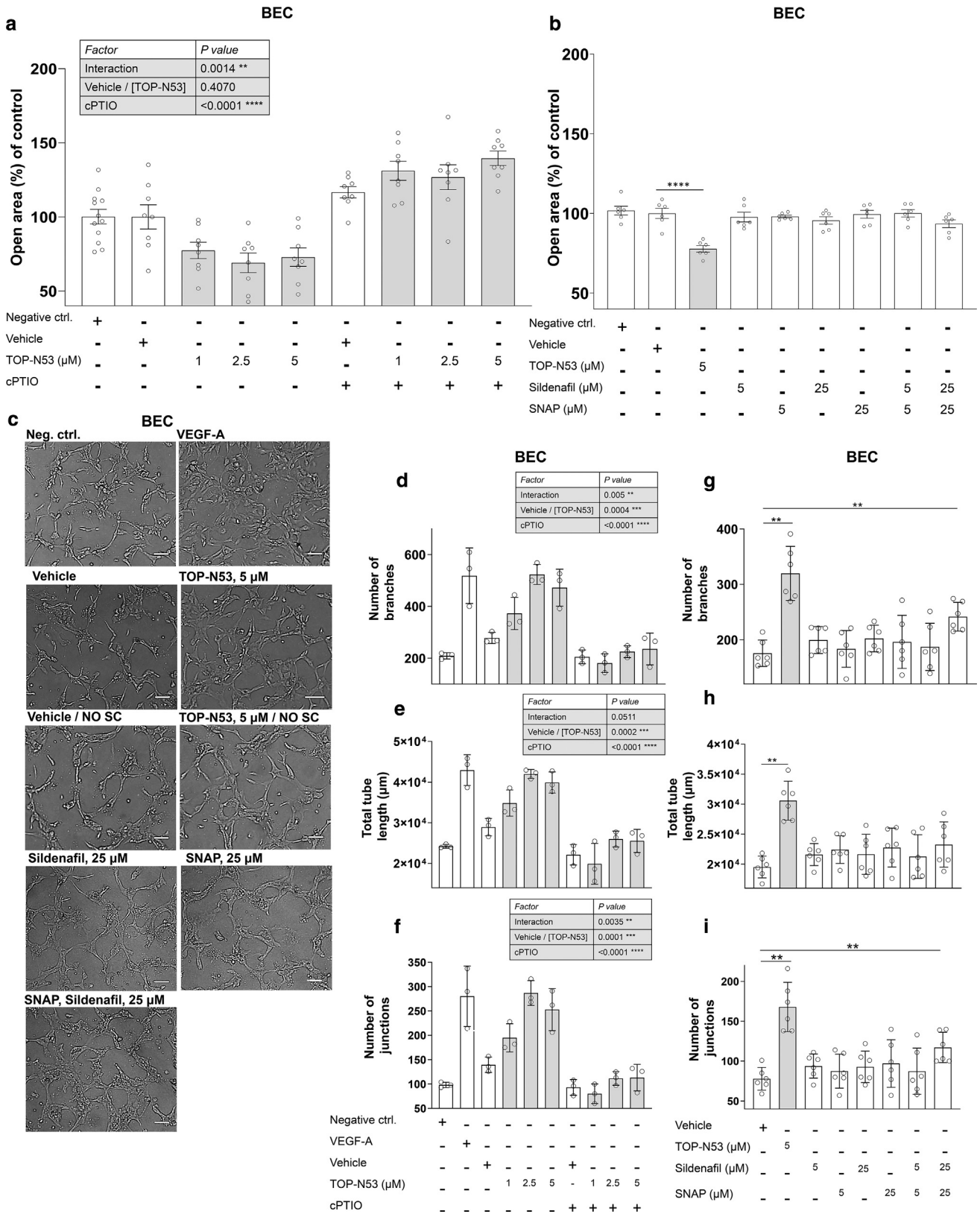


Figure 6. TOP-N53 promotes endothelial cell migration and tube formation. (a, b) Scratch wounding of primary human BEC treated for 6 h with TOP-N53 (a) in the presence or absence of cPTIO or (b) with sildenafil citrate and/or SNAP. n = 6–12 from one donor. (c–i) BEC were incubated for 16 hours in starvation medium (negative ctrl; VEGF-A positive ctrl) or (d–f) TOP-N53, (g–i) sildenafil, (g–i) SNAP, or (d–f) vehicle in the presence or absence of cPTIO. (c) Photomicrographs of the treated BEC, (d, g) number of branches, (e, h) total tube length, and (f, i) number of junctions. n = 3–6 from one donor. Bar = 100 μm. Statistical significance is only indicated for the TOP-N53, sildenafil, SNAP, and combined treatment of sildenafil and SNAP versus vehicle comparisons. BEC, blood endothelial cell; cPTIO, 2-(4-carboxyphenyl)-4,4,5,5-tetramethylimidazole-1-oxyl-3-oxide; ctrl, control; h, hour; SC, scavenger; SNAP, S-Nitroso-N-acetyl-DL-penicillamine.

morphogenesis had been reported for sildenafil (Pyriochou et al., 2007; Vidavalur et al., 2006). However, treatment with sildenafil or SNAP alone at the same or a five-fold higher concentration did not promote tube formation. The combined treatment with sildenafil and SNAP at a five-fold higher concentration had a significant effect but was still less efficient than TOP-N53 alone at a five-fold lower concentration.

Finally, we showed that TOP-N53 induces the expression of the proangiogenic factors *Vegfa* and *Hgf* (Brown et al., 1997; Bussolino et al., 1992; Ferrara, 1993) in cultured mouse primary fibroblasts (Supplementary Figure S6i and Figure 5h), whereas *Vegfa* expression in KCs was not affected (Supplementary Figure S6j). These results suggest that TOP-N53 promotes in vivo angiogenesis directly and also through fibroblasts.

In summary, TOP-N53 promoted several processes, which are compromised in chronic ulcers, including KC migration, angiogenesis, and GT formation. In addition, the dual activity of TOP-N53 is likely to promote the cutaneous vascular blood flow, which is frequently impaired in patients with chronic wounds (Eming et al., 2014). Our in vitro experiments strongly suggest that TOP-N53 is superior to previously used compounds that only release NO or only inhibit PDE5 because of its combined activity and its more pronounced and most likely more prolonged NO release. Therefore, the results presented in this study provide an exciting proof of concept for the therapeutic efficacy of TOP-N53 and encourage further translational research with optimized delivery systems and the clinical development of this compound for the treatment of nonhealing skin ulcers.

MATERIAL AND METHODS

Synthesis and use of TOP-N53

TOP-N53 was synthesized as described previously (Naef and Tenor, 2017). Two batches were used, which inhibited PDE5 enzymatic activity and increased cGMP levels in cellular assays with equal potency. The 10–100 mM solutions of TOP-N53 in 100% DMSO were diluted in 0.9% sodium chloride or cell culture media under sterile conditions. The final DMSO concentration was 0.01–0.05%.

Wound healing experiments

Mouse maintenance and animal experiments had been approved by the local veterinary authorities (Kantonales Veterinäramt Zurich, Switzerland). Full-thickness excisional wounds of 5 mm diameter were generated on the back of female C57BL/6JRj or male BKS(D)-Leprdb/JOrlR mice aged 9–11 weeks (Hiebert et al., 2018). Immediately after wounding, TOP-N53 or vehicle was injected intradermally at the wound edge, two injections per wound, and on treatment day at 25 μ l each. TOP-N53 of 0.00025 pmol or 0.001 pmol was injected (50 μ l of a solution of 5 pM TOP-N53 0.9% sodium chloride/0.01% DMSO) in healthy mice and 0.05 nmol or 0.2 nmol in mice with diabetes (50 μ l of a solution of 1 μ M TOP-N53 in 0.9% sodium chloride/0.01% DMSO). Wounds were allowed to heal without dressing.

Collagen and collagen cross-link analysis

Biochemical analysis of collagen and collagen cross-links in total wound lysates was performed as described previously (Hiebert et al., 2018).

Cell separation and flow cytometry

Flow cytometry analysis of wound tissue was performed as previously described (Haertel et al., 2018), with minor modifications (see Supplementary Materials and Methods).

Statistical analysis

Statistical analyses were performed using GraphPad Prism 7 or 8 software (GraphPad Software, La Jolla CA). Mann–Whitney *U* test was used for comparison of two groups. For analysis of wound closure, a two-sided Fisher's exact test was applied. To study TOP-N53 function in the presence of inhibitor, SNAP or sildenafil, a two-way ANOVA and Bonferroni multiple comparisons test were applied. Quantitative results are expressed as mean \pm SEM (* $P \leq 0.05$, ** $P \leq 0.01$, *** $P \leq 0.001$; **** $P \leq 0.0001$). Data from the key in vivo experiments were reproduced in at least two independent experiments, and data were combined in the graphs. The in vitro experiments were either performed in duplicate or more and/or repeated with other types of KCs (primary mouse vs. immortalized human KCs), fibroblasts (primary mouse vs. primary human fibroblasts), or endothelial cells (human umbilical vein endothelial cells vs. BEC) as stated in the text.

Data availability statement

No datasets were generated or analyzed during this study.

ORCID

Maya Ben-Yehuda Greenwald: <http://orcid.org/0000-0002-6089-0856>
Carlotta Tacconi: <http://orcid.org/0000-0002-6431-7555>
Marko Jukic: <http://orcid.org/0000-0002-5703-4573>
Natasha Joshi: <http://orcid.org/0000-0003-1275-0514>
Paul Hiebert: <http://orcid.org/0000-0001-8179-4217>
Jürgen Brinckmann: <http://orcid.org/0000-0001-6573-4783>
Hermann Tenor: <http://orcid.org/0000-0002-0867-2683>
Reto Naef: <http://orcid.org/0000-0002-7768-6026>
Sabine Werner: <http://orcid.org/0000-0001-7397-8710>

CONFLICT OF INTEREST

RN and HT are employees of Topadur Pharma AG (Schlieren, Switzerland), which owns TOP-N53. JB and SW have a consultancy relationship with Topadur Pharma AG. The remaining authors state no conflict of interest.

ACKNOWLEDGMENTS

We thank Rin Okumura, Hayley Hiebert (ETH Zurich, Switzerland), and Jaan Strang (Topadur Pharma AG) for technical assistance; Michael Cangkruma (ETH Zurich) for help with ear injections; Hans-Dietmar Beer (University of Zurich, Switzerland) for providing human primary foreskin KCs and fibroblasts; and Michael Detmar (ETH Zurich) for supervising the endothelial cell experiments and helpful suggestions. This work was supported by grants from the Commission for Technology and Innovation (grant 18271.1 PFLS-LS to SW and RN), Innosuisse (grant 29588.1 IP-LS to SW and RN), and the European Union (Eurostars project E!10192 to SW and HT). All correspondence regarding the TOP-N53 compound should be addressed to Dr Reto Naef (reto.naef@topadur.com).

AUTHOR CONTRIBUTIONS

Conceptualization: MBYG, RN, SW; Formal Analysis: MBYG, JB, HT; Funding Acquisition: SW, RN; Investigation: MBYG, CT, MJ, NJ, PH, JB, HT; Project Administration: SW; Supervision: SW; Visualization: MBYG; Writing - Original Draft Preparation: MBYG, SW; Writing - Review and Editing: MBYG, CT, MJ, NJ, PH, JB, HT, RN, SW

SUPPLEMENTARY MATERIAL

Supplementary material is linked to the online version of the paper at www.jidonline.org, and at <https://doi.org/10.1016/j.jid.2020.05.111>.

REFERENCES

- Brown LF, Detmar M, Claffey K, Nagy JA, Feng D, Dvorak AM, et al. Vascular permeability factor/vascular endothelial growth factor: a multifunctional angiogenic cytokine. *EXS* 1997;79:233–69.
- Bussolino F, Di Renzo MF, Ziche M, Bocchietto E, Olivero M, Naldini L, et al. Hepatocyte growth factor is a potent angiogenic factor which stimulates endothelial cell motility and growth. *J Cell Biol* 1992;119:629–41.

- Cai S, Khoo J, Mussa S, Alp NJ, Channon KM. Endothelial nitric oxide synthase dysfunction in diabetic mice: importance of tetrahydrobiopterin in eNOS dimerisation. *Diabetologia* 2005;48:1933–40.
- Campbell L, Saville CR, Murray PJ, Cruickshank SM, Hardman MJ. Local arginase 1 activity is required for cutaneous wound healing. *J Invest Dermatol* 2013;133:2461–70.
- Cash JL, Martin P. Myeloid cells in cutaneous wound repair. *Microbiol Spectr* 2016;4:385–403.
- Davis DW, Weidner DA, Holian A, McConkey DJ. Nitric oxide-dependent activation of p53 suppresses bleomycin-induced apoptosis in the lung. *J Exp Med* 2000;192:857–69.
- Dinh T, Veves A. Microcirculation of the diabetic foot. *Curr Pharm Des* 2005;11:2301–9.
- Edmonds ME, Bodansky HJ, Boulton AJM, Chadwick PJ, Dang CN, D'costa R, et al. Multicenter, randomized controlled, observer-blinded study of a nitric oxide generating treatment in foot ulcers of patients with diabetes—ProNOx1 study. *Wound Repair Regen* 2018;26:228–37.
- Eming SA, Martin P, Tomic-Canic M. Wound repair and regeneration: mechanisms, signaling, and translation. *Sci Transl Med* 2014;6:265sr6.
- Falanga V. Growth factors and chronic wounds: the need to understand the microenvironment. *J Dermatol* 1992;19:667–72.
- Farsaei S, Khalili H, Farboud ES, Khazaeipour Z. Sildenafil in the treatment of pressure ulcer: a randomised clinical trial. *Int Wound J* 2015;12:111–7.
- Ferrara N. Vascular endothelial growth factor. *Trends Cardiovasc Med* 1993;3:244–50.
- Gresele P, Momi S, Falcinelli E. Anti-platelet therapy: phosphodiesterase inhibitors. *Br J Clin Pharmacol* 2011;72:634–46.
- Gurtner GC, Werner S, Barrandon Y, Longaker MT. Wound repair and regeneration. *Nature* 2008;453:314–21.
- Haertel E, Joshi N, Hiebert P, Kopf M, Werner S. Regulatory T cells are required for normal and activin-promoted wound repair in mice. *Eur J Immunol* 2018;48:1001–13.
- Han G, Nguyen LN, Macherla C, Chi Y, Friedman JM, Nosanchuk JD, et al. Nitric oxide—releasing nanoparticles accelerate wound healing by promoting fibroblast migration and collagen deposition. *Am J Pathol* 2012;180:1465–73.
- Hemnes AR, Zaiman A, Champion HC. PDE5A inhibition attenuates bleomycin-induced pulmonary fibrosis and pulmonary hypertension through inhibition of ROS generation and RhoA/Rho kinase activation. *Am J Physiol Lung Cell Mol Physiol* 2008;294:L24–33.
- Hiebert P, Wietecha MS, Cangkrama M, Haertel E, Mavrogonatou E, Stumpe M, et al. Nrf2-mediated fibroblast reprogramming drives cellular senescence by targeting the matrisome. *Dev Cell* 2018;46:145–61.e10.
- Jamshidzadeh A, Azarpira N. The effects of topical sildenafil on wound healing in rat. *Iranian J Pharm Sci* 2011;7:43–8.
- Jones RE, Foster DS, Longaker MT. Management of chronic Wounds-2018. *JAMA* 2018;320:1481–2.
- Joost S, Zeisel A, Jacob T, Sun X, La Manno G, Lönnerberg P, et al. Single-cell transcriptomics reveals that differentiation and spatial signatures shape epidermal and hair follicle heterogeneity. *Cell Syst* 2016;3:221–37.e9.
- Kilic T, Parlakpinar H, Polat A, Taslidere E, Vardi N, Sarihan E, et al. Protective and therapeutic effect of molsidomine on bleomycin-induced lung fibrosis in rats. *Inflammation* 2014;37:1167–78.
- Kolluru GK, Bir SC, Kevil CG. Endothelial dysfunction and diabetes: effects on angiogenesis, vascular remodeling, and wound healing. *Int J Vasc Med* 2012;2012:918267.
- Krischel V, Bruch-Gerharz D, Suschek C, Kröncke KD, Ruzicka T, Kolb-Bachofen V. Biphasic effect of exogenous nitric oxide on proliferation and differentiation in skin derived keratinocytes but not fibroblasts. *J Invest Dermatol* 1998;111:286–91.
- Kulshrestha S, Chawla R, Alam MT, Adhikari JS, Basu M. Efficacy and dermal toxicity analysis of sildenafil citrate based topical hydrogel formulation against traumatic wounds. *Biomed Pharmacother* 2019;112:108571.
- Lee PC, Salyapongse AN, Bragdon GA, Shears LL, Watkins SC, Edington HD, et al. Impaired wound healing and angiogenesis in eNOS-deficient mice. *Am J Physiol* 1999;277:H1600–8.
- Lizarbe TR, García-Rama C, Tarín C, Saura M, Calvo E, López JA, et al. Nitric oxide elicits functional MMP-13 protein-tyrosine nitration during wound repair. *FASEB J* 2008;22:3207–15.
- Makrantonaki E, Wlaschek M, Scharffetter-Kochanek K. Pathogenesis of wound healing disorders in the elderly. *J Dtsch Dermatol Ges* 2017;15:255–75.
- Martin P. Wound healing—aiming for perfect skin regeneration. *Science* 1997;276:75–81.
- Masters KSB, Leibovich SJ, Belem P, West JL, Poole-Warren LA. Effects of nitric oxide releasing poly(vinyl alcohol) hydrogel dressings on dermal wound healing in diabetic mice. *Wound Repair Regen* 2002;10:286–94.
- Murohara T, Witzenbichler B, Spyridopoulos I, Asahara T, Ding B, Sullivan A, et al. Role of endothelial nitric oxide synthase in endothelial cell migration. *Arterioscler Thromb Vasc Biol* 1999;19:1156–61.
- Naef R, Tenor H. 2-phenyl-3, 4-dihydropyrrolo 2018;2:[1, 2, 4] triazinone derivatives as phosphodiesterase inhibitors and uses thereof. *Google Patents*, https://patentscope.wipo.int/search/en/detail.jsf?docId=WO2017085056&_cid=P22-KCKW9Z-24934-1; 2017 (accessed 15 July 2020).
- Okonkwo UA, DiPietro LA. Diabetes and wound angiogenesis. *Int J Mol Sci* 2017;18:1419.
- Pyriochou A, Zhou Z, Koika V, Petrou C, Cordopatis P, Sessa WC, et al. The phosphodiesterase 5 inhibitor sildenafil stimulates angiogenesis through a protein kinase G/MAPK pathway. *J Cell Physiol* 2007;211:197–204.
- Schwentker A, Billiar TR. Nitric oxide and wound repair. *Surg Clin North Am* 2003;83:521–30.
- Sen CK, Gordillo GM, Roy S, Kirsner R, Lambert L, Hunt TK, et al. Human skin wounds: a major and snowballing threat to public health and the economy. *Wound Repair Regen* 2009;17:763–71.
- Sennett R, Wang Z, Rezza A, Grisanti L, Roitershtein N, Sicchio C, et al. An integrated transcriptome atlas of embryonic hair follicle progenitors, their niche, and the developing skin. *Dev Cell* 2015;34:577–91.
- Stallmeyer B, Kämpfer H, Kolb N, Pfeilschifter J, Frank S. The function of nitric oxide in wound repair: inhibition of inducible nitric oxide-synthase severely impairs wound reepithelialization. *J Invest Dermatol* 1999;113:1090–8.
- Tsuboi R, Rifkin DB. Recombinant basic fibroblast growth factor stimulates wound healing in healing-impaired db/db mice. *J Exp Med* 1990;172:245–51.
- Vidavalur R, Penumathsa SV, Zhan L, Thirunavukkarasu M, Maulik N. Sildenafil induces angiogenic response in human coronary arteriolar endothelial cells through the expression of thioredoxin, hemeoxygenase and vascular endothelial growth factor. *Vascul Pharmacol* 2006;45:91–5.
- Wang R, Ghahary A, Shen YJ, Scott PG, Tredget EE. Nitric oxide synthase expression and nitric oxide production are reduced in hypertrophic scar tissue and fibroblasts. *J Invest Dermatol* 1997;108:438–44.
- Weller R, Finnen MJ. The effects of topical treatment with acidified nitrite on wound healing in normal and diabetic mice. *Nitric Oxide* 2006;15:395–9.
- Werner S, Grose R. Regulation of wound healing by growth factors and cytokines. *Physiol Rev* 2003;83:835–70.
- Werner S, Krieg T, Smola H. Keratinocyte—fibroblast interactions in wound healing. *J Invest Dermatol* 2007;127:998–1008.
- Witte MB, Kiyama T, Barbul A. Nitric oxide enhances experimental wound healing in diabetes. *Br J Surg* 2002a;89:1594–601.
- Witte MB, Thornton FJ, Tantry U, Barbul A. L-arginine supplementation enhances diabetic wound healing: involvement of the nitric oxide synthase and arginase pathways. *Metabolism* 2002b;51:1269–73.
- Yamasaki K, Edington HD, McClosky C, Tzeng E, Lizonova A, Kovesdi I, et al. Reversal of impaired wound repair in iNOS-deficient mice by topical adenoviral-mediated iNOS gene transfer. *J Clin Invest* 1998;101:967–71.
- Zhan R, Yang S, He W, Wang F, Tan J, Zhou J, et al. Nitric oxide enhances keratinocyte cell migration by regulating Rho GTPase via cGMP-PKG signalling. *PLoS One* 2015;10:e0121551.
- Ziche M, Morbidelli L, Masini E, Amerini S, Granger HJ, Maggi CA, et al. Nitric oxide mediates angiogenesis in vivo and endothelial cell growth and migration in vitro promoted by substance P. *J Clin Invest* 1994;94:2036–44.